J. Mol. Biol. (1997) **273**, 467–478

JMB

Mutant ATP-binding RNA Aptamers Reveal the Structural Basis for Ligand Binding

Thorsten Dieckmann[1], Samuel E. Butcher[1], Mandana Sassanfar[2] Jack W. Szostak[2] and Juli Feigon[1]*

[1]*Department of Chemistry and Biochemistry and the Molecular Biology Institute, University of California at Los Angeles 405 Hilgard Ave, Los Angeles CA 90095, USA*

[2]*Department of Genetics Harvard Medical School and Department of Molecular Biology, Massachusetts General Hospital, Boston, MA 02114 USA*

**Corresponding author*

The solution structure of the ATP-binding RNA aptamer has recently been determined by NMR spectroscopy. The three-dimensional fold of the molecule is determined to a large extent by stacking and hydrogen bond interactions. In the course of the structure determination it was discovered that several highly conserved nucleotides in the binding pocket can be substituted while retaining binding under NMR conditions. These surprising findings allow a closer look at the interactions that determine stability and specificity of the aptamer as well as local structural features of the molecule. The binding properties of ATP binder mutants and modified ligand molecules are explored using NMR spectroscopy, column binding studies and molecular modeling. We present additional evidence and new insights regarding the network of hydrogen bonds that defines the structure and determines stability and specificity of the aptamer.

Keywords: NMR; RNA structure; binding constants; RNA folding; *in vitro* selection

Introduction

RNA aptamers selected for binding to biological cofactors are useful model systems to explore structural motifs that might have been of importance during the hypothetical RNA-world. Recently, the first structures of RNA aptamers identified *via in vitro* selection (Ellington & Szostak, 1990; Tuerk & Gold, 1990) to bind selectively the metabolic cofactors ATP and FMN (Lauhon & Szostak, 1995; Sassanfar & Szostak, 1993) as well as the amino acids citrulline and arginine (Famulok, 1994) were solved using NMR spectroscopy (Dieckmann *et al.*, 1996; Fan *et al.*, 1996; Jiang *et al.*, 1996b; Yang *et al.*, 1996).

The structure of the ATP-binding RNA aptamer (Dieckmann *et al.*, 1996; Jiang *et al.*, 1996b) revealed how RNA can form a well-defined binding pocket capable of recognizing and binding the adenosine moiety of ATP and NAD with high affinity and specificity. The RNA–ligand interaction takes place in an internal loop region of the aptamer that is flanked by two stems and opposite a single bulged guanine residue (Figure 1). Two asymmetric G·G base-pairs (G7·G11 and G17·G30) cap the stems and form the foundation of the binding pocket by providing an interface for the stacking of the internal loop residues and the stems (Figure 2). The stacking of the first stem is continued by the G7·G11 and G8·ATP base-pairs and closed by a U-turn motif, which includes the ATP in a GNRA tetraloop-like arrangement (G8, A9, A10 and AMP). The second stem continues into the internal loop *via* the G17·G30 base-pair and a partial stacking of U16 and A12 on the G·G base-pair. The nucleotides A13, A14, and C15 form a continuous stack and function as a linker in the back of the binding pocket. The ATP is hydrogen bonded *via* its amino group and N1 to G8 and *via* its N3 to A12. Another important interaction involves the 2′ hydroxyl group of G30, which forms a hydrogen bond with the N7 of A12.

Obtaining the assignments for the NMR structure determination of this aptamer-AMP complex was extremely challenging (Dieckmann & Feigon, 1997; Jiang *et al.*, 1996a), mostly due to its relatively large size and its unpredictable three-dimensional fold. In order to resolve ambiguities in the assignments and NOE connectivities, several aptamers

Abbreviations used: NOE, nuclear Overhauser enhancement; NOESY, NOE spectroscopy; TOCSY, total correlated spectroscopy; DFQ-COSY, double quantum-filled COSY; HSQC, heteronuclear single quantum coherence; FID, free induction decay; TPPI, time proportional phase incrementation; 2D, two-dimensional; ppm, parts per million.

0022–2836/97/420467–12 $25.00/0/mb971329

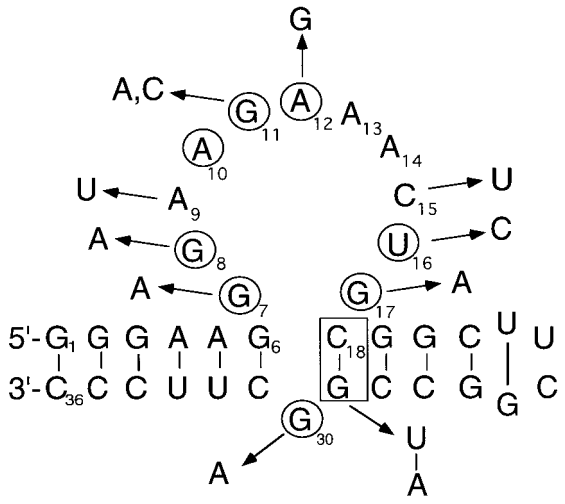

Figure 1. Sequence and secondary structure of the ATP-binding RNA aptamer. Base substitutions used in this study are labeled next to the original (wild-type) nucleotides. Nucleotides that were conserved in all the clones are circled.

with base substitutions were also studied by NMR spectroscopy. This led to the finding that base substitutions at several of the completely conserved nucleotides in the consensus sequence of the ATP-binding RNA aptamer were tolerated, i.e. binding to the AMP was still detected under NMR conditions (Dieckmann *et al.*, 1996). In order to gain further insight into the interactions between the AMP and the RNA as well as the basis of the folding and stability of the aptamer we have investigated the binding properties of mutant aptamers by NMR, ATP-binding assays, and molecular modeling. The mutant aptamers allow a closer investigation of local interactions within the aptamer structure. Of special interest are the importance of hydrogen bond and stacking interactions with respect to the binding specificity and stability of the complex.

Results and Discussion

Evaluation of binding properties of aptamers by NMR spectroscopy

The binding of AMP to the wild-type and mutant aptamers shown in Figure 1 was qualitatively assessed by observation of changes in the imino proton spectra as a function of added AMP to ~1 mM RNA samples at 274 K. The chemical shifts and line-widths in the imino and aromatic proton regions of the mutant aptamer spectra with different RNA:AMP ratios were compared with each other and with the spectra of the original aptamer in the absence and presence of AMP. For the original aptamer used in the structural studies, one-dimensional ^{1}H NMR spectra of the RNA in water exhibit imino resonances for the stem nucleotides and UUCG loop only. Upon addition of AMP, additional resonance intensity corresponding to imino protons in the internal loop and bulged G30 is observed, indicative of the bound conformation (Dieckmann *et al.*, 1996; Jiang *et al.*, 1996b).

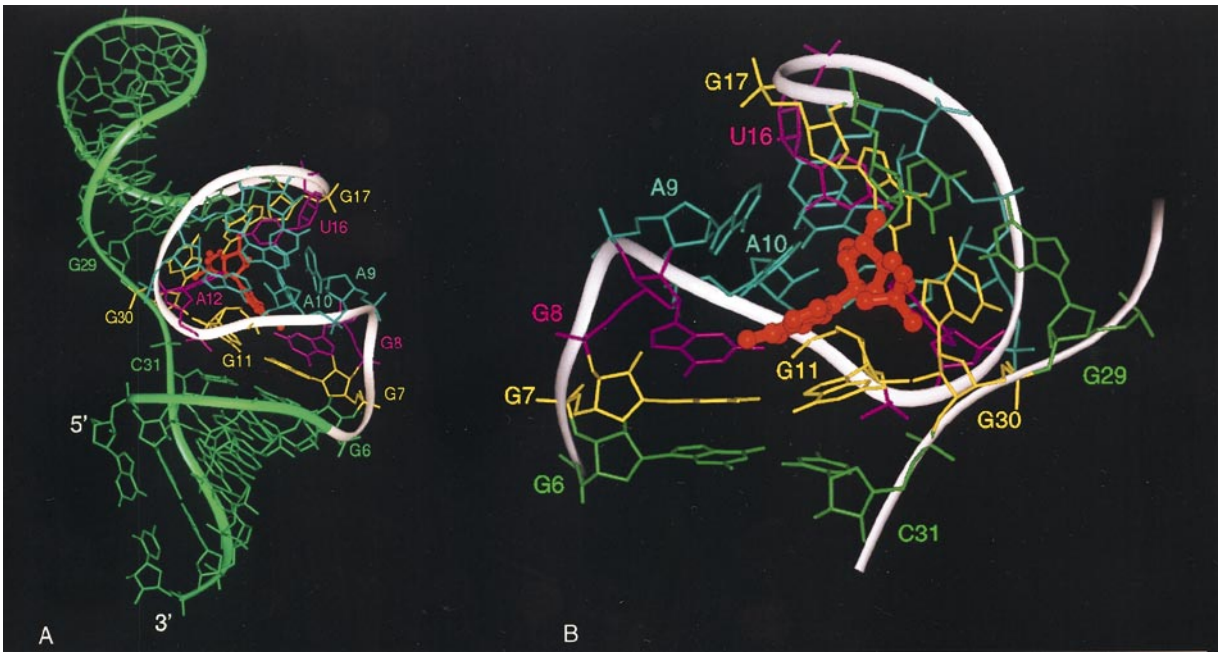

Figure 2. Three-dimensional structure of the ATP-binding RNA aptamer. (a) View of the whole molecule including the A-form stems. (b) View of the core of the aptamer (nucleotides 6 to 18, 29 to 31, and AMP). The stem base-pairs are shown in green, the G·G base-pairs in yellow, nucleotides interacting with the AMP in purple (G8, A12, U16), and the connecting nucleotides in GNRA motif and linker are in blue.

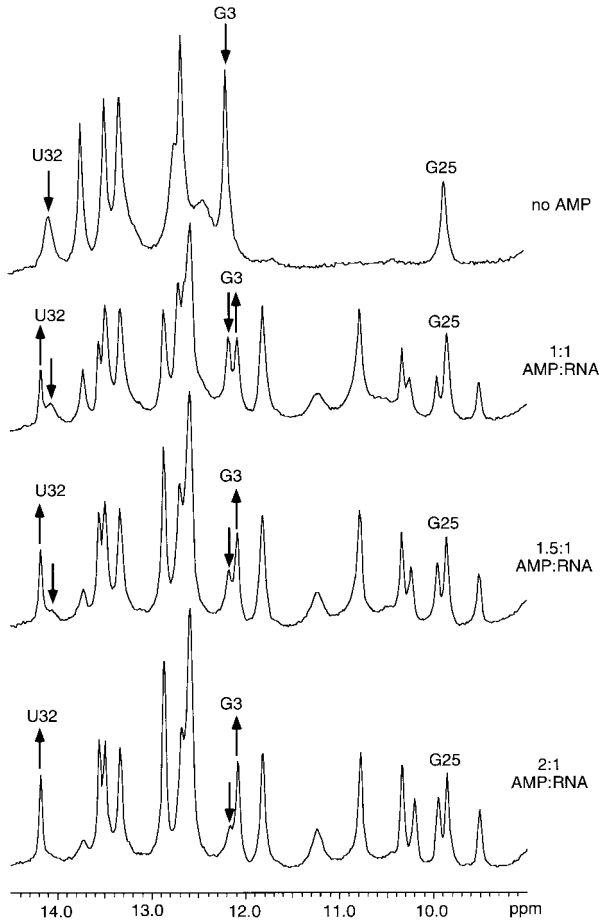

Figure 3. One-dimensional ^{1}HNMR spectra of the exchangeable resonances of the G8A mutant aptamer at different AMP:RNA ratios. The spectra were measured at 274 K on a sample containing 0.8 mM RNA in 100 mM NaCl (pH 6.0). For each spectrum 128 scans of 4,096 complex points were acquired. The FIDs where zero-filled to 16 K and transformed after multiplication with an exponential function (LB = 15).

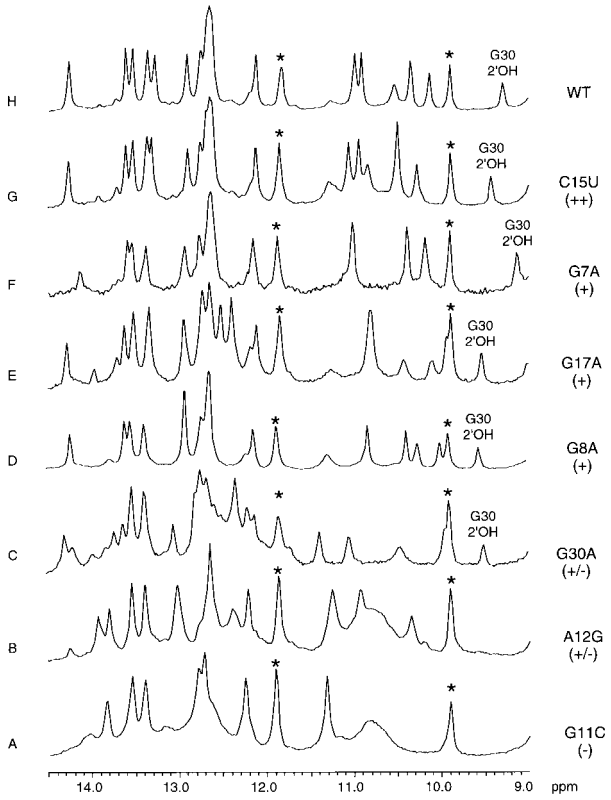

Figure 4. One-dimensional ^{1}HNMR spectra of the exchangeable resonances of wild-type aptamer (WT) and several mutant aptamers in the presence of an excess of AMP (10 to 100%). The spectra were measured at 274 K on a samples containing 0.5 to 1.2 mM RNA in 100 mM NaCl (pH 6.0). For each spectrum 128 scans of 4,096 complex points where acquired. The FIDs where zero-filled to 16 K and transformed after multiplication with an exponential function (LB = 15). The imino resonances from the U22·G25 wobble pair are indicated by *.

Figure 3 shows the results of a titration of the G8A mutant with AMP. As is the case for the original aptamer, additional exchangeable resonances appear upon addition of AMP. However, in this case some resonances shift and/or change line-widths as a function of added AMP. In contrast to the original aptamer, the G8A mutant does not completely exist as an AMP:RNA complex at a 1:1 AMP:RNA ratio (0.8 mM), but still contains ~50% unbound RNA. However, at AMP:RNA ratios of 2:1 or higher the complex predominates.

Typical one-dimensional spectra for various mutants in the presence of AMP are shown in Figure 4. The binding of the mutant aptamers under NMR conditions was classified as follows: aptamers that did not show any changes in their peak patterns and line-widths independent of the amount of AMP present were classified as ''non-binding'' aptamers (−) (G11A, G11C). These RNAs have NMR spectra with features very similar to the wild-type aptamer in the absence of AMP and in some cases (e.g. G11C) show additional resonance intensity from protons in the internal loop (Figure 4 (a)). Mutant aptamers that showed additional signals and/or changes in line-widths upon addition of AMP, but did not convert into a fully bound complex at any AMP concentration, were classified as weak binders (+/−) (A12G, U16C, G30A). Mutants classified as (+/−) show broad and additional lines compared to the original aptamer (Figure 4 (b) and (c)). In the case of aptamers that could be converted to more than 90% RNA:AMP complex, additional 2D spectra were acquired to further evaluate the binding properties and the structures. The spectra were checked for the presence of NOE patterns characteristic of the structure of the original aptamer complex. The crosspeaks of A12 were especially useful in this respect, as A12 is located in the core of the aptamer and interacts directly with the ligand. A12 shows very distinctive NOE patterns and chemical shifts for its base H2, H8 and amino resonances. Spectra were also analyzed for any

Table 1. Summary of binding data for the ATP-binding aptamer and mutants as assayed by NMR, in vitro selection conditions, and isocratic elution off an AMP-agarose column.

Mutation	NMR binding	*In vitro* selection binding[a]	k_D (μM)	$\Delta\Delta G$[b] (kcal/mol)
WT	++	+	0.8	–
G7A	+	n.d.	150	3.0
G8A	+	–	115	2.9
A9U	++	n.d.	n.d.	–
G11C	–	–	n.d.	–
G11A	–	n.d.	n.d.	–
A12G	+/–	n.d.	n.d.	–
C15U	+	–	n.d.	–
U16C	+/–	–	⩾170	⩾3.1
G17A	+	–	98	2.8
G30A	+/–	n.d.	n.d.	–
C18U/G29A	++	+	14 [b]	1.6

n.d., not determined.
[a] Aptamer elutes from column in wash (–); aptamer is retained on column and eluted with ATP (+).
[b] Apparent $\Delta\Delta G$ of mutant *versus* original aptamer at 293 K.
[c] From Sassanfar & Szostak (1993).

signs of exchange between the free and bound forms of AMP (e.g. exchange peaks for AMP H2 and H8 in NOESY spectra) over the temperature range in which the original aptamer:AMP complex is stable (273 to 313 K). Aptamers that showed signs of exchange at temperatures less than 313 K but displayed all the characteristics of a fully bound complex were classified as good AMP binders (+) (G7A, G8A, G17A, C15U) (Figure 4 (d), (e), (f) and (g)). Those mutant aptamers that behave in all aspects like the original sequence were classified as ''wild-type''-like binders (++) (A9U, C18U/G29A). As can be seen in Figure 4, aptamers classified as (+) and (++) exhibit the same features in the one-dimensional spectra as the original aptamer. The presence of the G30 2′ OH signal at ~9.2 ppm is characteristic of the formation of a wild-type-like complex. All mutants and their qualitative NMR binding classifications are summarized in Table 1.

Analysis of the NOESY spectra of the mutant aptamers indicates that all mutant aptamers that form stable complexes with AMP (those of types + and ++) must have structures very similar to the original aptamer. In all these cases, the observed NOE patterns show that the stacking arrangement and the orientation of the bound ligand are retained.

Mutant aptamers that form stable complexes under NMR conditions do not all bind ATP under *in vitro* selection conditions

The observation that some of the aptamers with base substitutions at absolutely conserved positions still formed stable folded complexes with AMP led us to ask why none of the mutant aptamers showed up in any of the selections; i.e. was sequence space inadequately sampled during the selection and/or cloning, or would these sequences have been excluded by the stringency of the selection conditions? In order to answer this question, aptamers from each of the NMR-derived classes of binding properties (–, +/–, +, and ++) were tested for binding to an ATP–agarose column under the same conditions as were used in the original selection experiment (Sassanfar & Szostak, 1993). All of the aptamers classified as –, +/–, and + eluted from the column in the 5 ml wash and thus would not have been selected for (Table 1). These include the mutant aptamers G7A, G8A, G17A, and C15U, which form stable and well structured complexes under NMR conditions. Of the aptamers tested for binding, only the original aptamer and the C18U/G29A double substitution bind to the column and are eluted with the ATP-containing buffer. The C18U/G29A substitution corresponds to a sequence present in the original selection and these bases are not part of the conserved sequence. The A9U mutant, which also shows wild-type binding (++) as assayed by NMR, is the only other mutant studied here with a mutation in a non-conserved base. A9 is the N base in the GNRA tetraloop, and thus serves a role only as a spacer nucleotide. These results show that none of the aptamers with base substitutions in the conserved positions would have survived the *in vitro* selection process, because they would have been eliminated during the first one or two rounds of *in vitro* selection.

Base substitutions that show binding retain the same global fold

It was initially surprising to find that some aptamers with base substitutions in conserved bases still showed binding to AMP under NMR conditions. This was particularly the case for the G8A mutant, since the refined structure reveals that G8 base-pairs with the AMP *via* two hydrogen bonds.

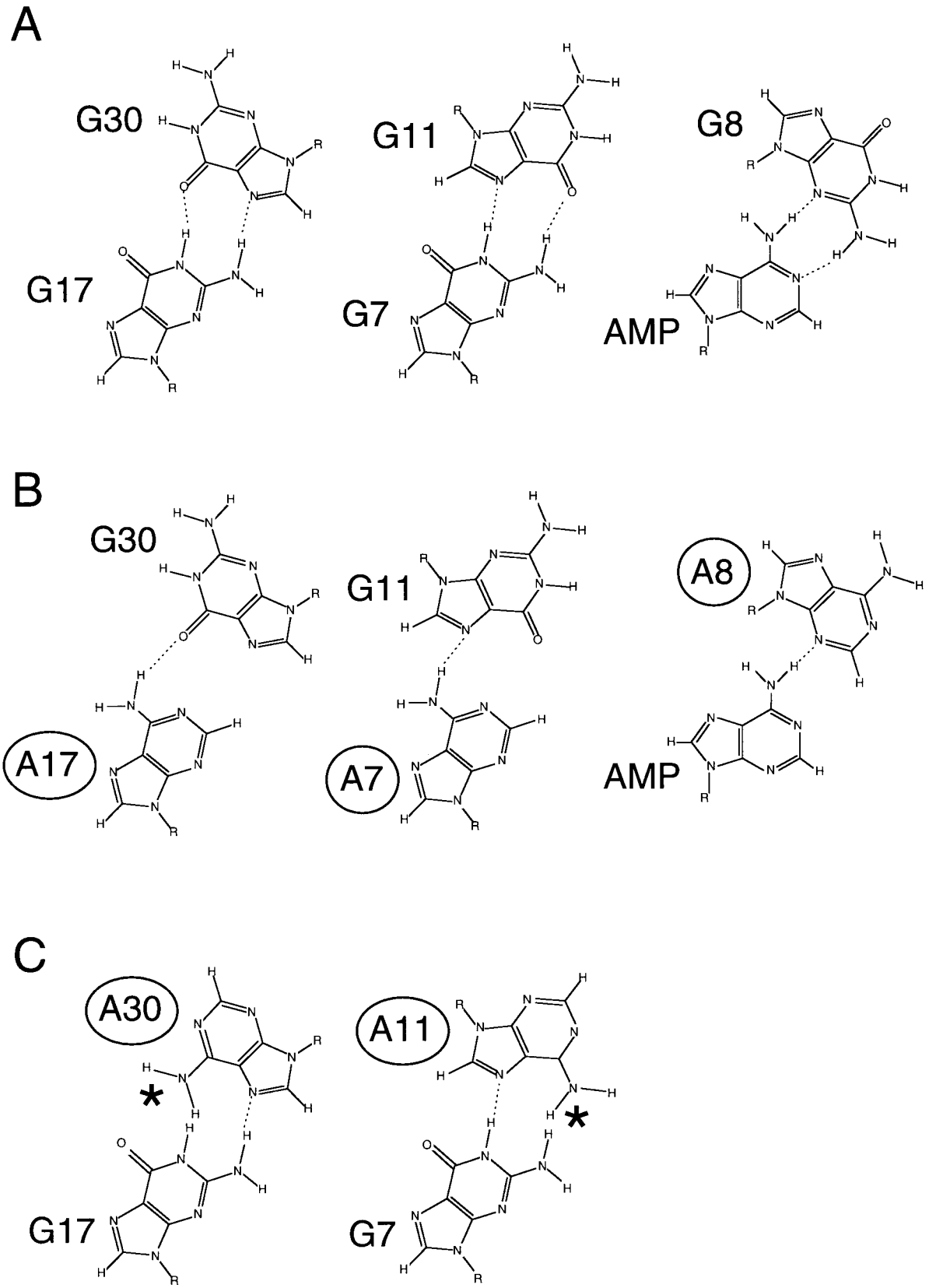

Figure 5. (a) G·G and G·A base-pairs in wild-type aptamer and the possible base-pairing arrangements in the mutant aptamers (b) G17A, G7A, G8A and (c) G30A, G11A. The stars in C highlight the positions where steric clashes would interfere with base-pair formation.

The two G·G base-pairs that cap the two stems of the aptamer each tolerate a substitution of one G for an A but not the other. For the G7·G11 base-pair, a G7A substitution retains the binding capabilities, whereas a G11A substitution does not. The G17·G30 base-pair can be replaced by A17·G30 (G17A mutant), but not by G17·A30 (G30A mutant). In the latter case the complex stability is greatly reduced.

Molecular modeling was used to assess how well the base substitutions fit into the structural framework of the original ATP-binder structure. Figure 5(a) shows the G7·G11, G8·AMP, and G17·G30 base-pairing interactions found in the wild-type aptamer structure. For the three aptamers that contain mutations in these conserved nucleotides (G17A, G7A, and G8A), the substituted A base can be accommodated in the same position as the wild-type G, albeit with the loss of one hydrogen bond interaction (Figure 5(b)). Consistent with this, these mutants still show binding under NMR conditions. The loss of a hydrogen bond would explain the reduced stability while the maintenance of the stacking interactions would explain why these mutations still allow proper folding and binding. In contrast, for the case of the G30A and G11A mutants, positioning the substituted A residue in the same place as the G residues would lead to steric clash between pairs of amino groups (G11A mutant) or the A amino and G imino groups (G30A mutant) (Figure 5(c)). Thus, modeling would lead to the prediction that these mutants would not form a stable complex. This is consistent with the greatly decreased level of binding by G30A and the absence of binding by G11A mutants as assayed by NMR.

In the wild-type ATP-binding aptamer, the A12 amino hydrogen bonds to the AMP N3. The position of A12 is further stabilized by a hydrogen bond between the A12 N7 and the G30 2′ OH (Figure 2). For the A12G mutant, substitution of G12 for A12 would result in loss of the hydrogen bond between the A amino and AMP N3, which at least partially explains the decrease in binding for this +/− mutant. However, by itself it probably does not explain the almost complete loss of binding, since the case of the G8A mutant shows that a loss of one hydrogen bond interaction can be tolerated if the overall structure is retained. The A12G model structure suggests one possible explanation; a guanine in position 12 is nicely oriented to form a hydrogen bond between its amino group and the O6 of G17, or with a small repositioning a symmetrical G12·G17 base-pair; thus the strongly reduced binding and spectra in intermediate exchange can be due to the formation of an alternative, more stable structure involving a G·G interaction. This is supported by the fact that even though the spectra show some of the characteristic changes indicative of complex formation upon the addition of AMP, there is no evidence for the G30 2′ OH resonance, which is consistent with a different orientation of G30 relative to G12.

Dissociation constants of the mutant aptamers give insights into the involved interactions

In order to obtain more quantitative information about the binding of those mutants that form stable and specific AMP–aptamer complexes under NMR conditions, k_D values were measured using isocratic elution. The values determined are summarized in Table 1. All mutant aptamers tested have dissociation constants of ~100 μM or higher, except for the stem double mutant C18U/G29A, which has a k_D of 14 μM. This is in agreement with the results from the *in vitro* selection binding studies, as only aptamers with binding constants lower than 80 μM can survive under the selection conditions (based on column size and volume of wash). The k_D values are consistent with the initial classification by NMR, i.e. mutants with k_D values of 14 μM or less form a fully bound complex at 1:1 RNA:ligand ratio (type ++) and mutants with k_D values of 100 to 150 μM (type +) can still be driven towards a completely bound complex under NMR conditions at higher RNA concentration (~1.0 mM). It should be noted that the ATP binding has different k_D values in solution and on the affinity column. For the original consensus aptamer, the k_D for binding immobilized ATP was 14 μM compared with a solution k_D of 6 to 8 μM determined by equilibrium gel filtration (Sassanfar & Szostak, 1993). Thus it is likely that the dissociation constants of all ATP-binding aptamers are up to a factor of 2 smaller under NMR conditions than those reported here determined by column binding.

Compared to the wild-type aptamer, the apparent dissociation constants of 100 to 200 μM for the mutants correspond to a difference in the free energy of complex formation ($\Delta\Delta G_{complex}$) of ~3.0 kcal/mol at 293 K (1.6 kcal/mol for the C18U/G29A mutant), as calculated from:

$$\Delta\Delta G_{complex} = -RT \ln(k_D^{orig}/k_D^{mutant})$$

The $\Delta\Delta G$ value found for the C18U/G29A stem mutation is close to the difference found for the removal of one hydrogen bond in the closing stem G·C base-pair of the 5′-GG**C**[GCAA]**G**CC tetraloop (SantaLucia *et al.*, 1992). Thus it seems likely that the observed difference in ATP binding is mostly due to the reduced stability (two hydrogen bonds in A·U *versus* three hydrogen bonds in G·C) of the closing stem base-pair, which forms the stacking platform for the G30·G17 base-pair. However, for the mutations within the core of the aptamer, loss of a single hydrogen bond interaction is probably not sufficient to explain the difference in free energies of complex formation (SantaLucia *et al.*, 1992; Turner *et al.*, 1987; and see Figure 5). Changes in the stacking interactions between bases and perhaps other unidentified hydrogen bonds must contribute to the reduced complex stability. For the G8A mutant, it is clear from the NOE data and modeling studies that the G can be replaced

by A without any change in the positioning of the base while retaining the AMP amino to G8 N3 H-bond (Fig. 5B). In addition to this interaction with the ligand, the G8 is also part of the U-turn motif and is positioned in place of the first G in a GNRA tetraloop-like arrangement. Previous investigations of this type of tetraloop provide evidence for a hydrogen bond from the G imino group to the $n + 3$ phosphate oxygen atom (Heus & Pardi, 1991; Jucker *et al*., 1996; Jucker & Pardi, 1995; SantaLucia *et al*., 1992). The NMR data and structure of the ATP-binding aptamer are also consistent with formation of this hydrogen bond. Thus the change of a guanine in position 8 to an adenine will also result in a deletion of an additional hydrogen bond. The removal of these two interactions can explain the observed $\Delta\Delta G$ value. No obvious secondary H-bond interactions are known for the bases of the two G·G base-pairs. However, minor rearrangements with respect to the base position and stacking interactions are likely upon substitution of adenine for G8 or G7, in order for at least one hydrogen bond from the base-pair to be retained (Figure 5). Thus the observed ΔG values could correspond to the loss of one hydrogen bond plus an additional penalty for less-perfect stacking.

An all-DNA version of the aptamer does not bind ATP

In order to assess the importance of RNA *versus* DNA nucleotides in the structure of the ATP binding aptamer, aptamers of the same sequence containing all deoxyribose nucleotides and deoxyribonucleotide substitutions in the non-conserved stem regions only, as well as single deoxyribose substitutions (Table 2; discussed below), were synthesized. These were tested for ATP binding using isocratic elution off an ATP–agarose column as discussed above for the base mutants. No detectable binding was found for the all-DNA version of the ATP-binding RNA aptamer ($k_D > 1$ mM). For the aptamer with DNA substitutions for all the base-pairs in the stems except the ones flanking the internal loop, the binding of ATP was decreased by a factor of 20 ($k_D = 0.3$ mM) compared to the all-RNA version. This implies that even though the stems do not form part of the binding pocket, an A-form helix is essential to position the G·G base-pairs at the correct angle for the stacking interactions that stabilize the binding pocket.

Several 2′ hydroxyl interactions seem to be crucial for a stable structure

Hydrogen bonds are clearly of great importance for the stability and specificity of the ATP-aptamer complex. In addition to base-pairing interactions, there is evidence from the structures and NMR data that the 2′ hydroxyl groups of G30, G8 and the AMP participate in hydrogen bonds as donors or acceptors. In most cases, evidence for the participation of the 2′ OH in hydrogen bonds is indirectly obtained from the structure, since the resonance from the 2′ OH usually exchanges too fast and/or overlaps with too many resonances to be observed. The G30 2′ OH is an exception, because it is unusually down-field shifted (~9.2 ppm) and slowly exchanging. On the basis of the NMR structure and nitrogen chemical shifts, G30 2′ OH hydrogen bonds with A12 N7.

Table 2. Effect of deoxyribonucleotide substitutions on ATP binding

Deoxyribonucleotide substitution	ATP binding[a]
G7	+
G8	−
A9	+
A10	+
G11	+
A12	+
A13	+
A14	+
C15	+
U16	+
G17	+
G30	−
All DNA[b]	− ($k_D > 1$ mM)
Stems DNA[b] (1–5, 20–33, 35–40)	− ($k_D = 300$ μM)

[a] +, Binding is comparable to the original consensus aptamer; −, no or greatly decreased binding.
[b] Modifications of the original 40-mer sequence (Sassanfar & Szostak, 1993).

Further evidence for the importance of this G30 2′ OH H-bond was obtained from binding studies on aptamers containing deoxyribose substitutions. Aptamers containing single deoxyribose substitutions were made for all of the nucleotides that are part of the binding pocket. The binding results are listed in Table 2. A single deoxyribose substitution in position 8 or 30 eliminates AMP/ATP binding. All other ribonucleotides in the internal loop can be exchanged one by one against deoxyribonucleotides without major effects with respect to the binding properties.

G8 is located at the base of the GNRA-like tetraloop. In this case the 2′ OH is not directly observed by NMR, but both the structure and the nitrogen chemical shift are consistent with an H-bond from the G8 2′-hydroxyl group to the N7 of A10, the R base in the GNRA motif. Evidence for this hydrogen bond is also present in other GNRA and U-turn motifs (Heus & Pardi, 1991; Jucker & Pardi, 1995). The deoxyribose substitution at G8 probably affects ATP binding by destabilizing the tetraloop motif that forms a central feature of the binding pocket for the ATP.

Except for the ATP (discussed below), there is no NMR, chemical, or other evidence for any other important 2′ OH interactions in the binding pocket of the aptamer. This is an interesting point, since it

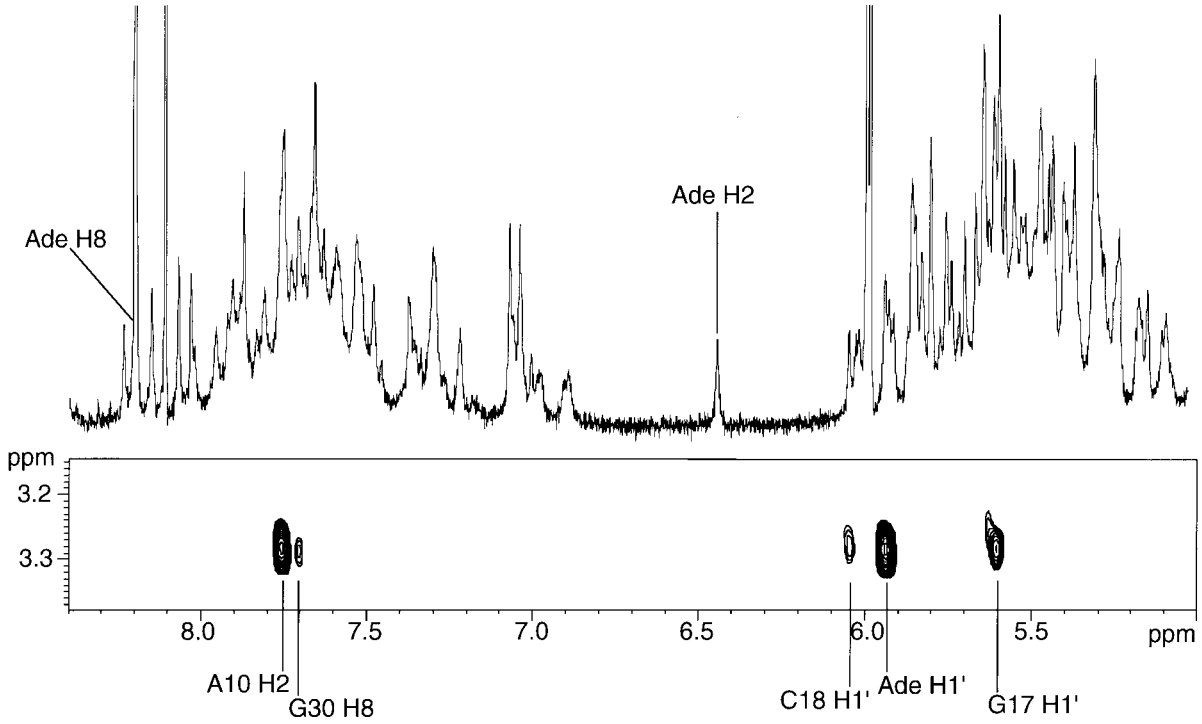

Figure 6. (a) One-dimensional spectrum and (b) strip of 2D NOESY spectrum of the wild-type aptamer in complex with 2′-*O*-Me-adenosine in ^2H_2O. The strip in (b) was taken at the frequency of the methyl group of the 2′-*O*-Me-adenosine. Spectra were acquired at 293 K. For (a) 128 scans of 8 K complex points were acquired. The FID was zero-filled to 16 K and transformed after multiplication with a 60 degree shifted squared sine-bell. The 2D spectrum in (b) was acquired with 96 scans per t_1 increment using States-TPPI phase cycling. 256 and 1024 complex points were acquired in the f_1 and f_2 dimensions, respectively. The final data matrix was 2,048 × 2,048 points and was processed with a Gaussian filter function (LB, 18, GB, 0.08 in f_2 and 0.14 in f_1).

has been widely thought that the 2′ OH of RNA provides additional functional groups *versus* DNA to allow RNA to act as a catalyst and to form a wider variety of folded structures. In this case, the majority of the 2′ hydroxyl groups do not appear to play any role in the structure of the aptamer. On the other hand, the few 2′ hydroxyl groups that are involved in hydrogen bonds are essential to the stability of the structure.

Importance of the AMP 2′ OH

A variety of modified nucleotides was tested for binding to the ATP-binding aptamer (Sassanfar & Szostak, 1993). It was found that substitution of dATP for ATP eliminates binding, which suggests that the 2′ hydroxyl group of the ligand plays an essential role in binding. On the basis of distances and angles between acceptor and donor atoms in the NMR structure, we proposed several possible interactions for the AMP 2′ OH group, including G30 N7, A12 N1 and G17 N3 (Dieckmann *et al.*, 1996). A closer look at the biochemical data, especially the study of the binding properties of ATP derivatives (Sassanfar & Szostak, 1993), reveals that although deoxyribo ATP does not bind to the aptamer, 2′-*O*-Me-AMP does bind, albeit with reduced affinity. This strongly suggests that the 2′ O acts as an acceptor atom rather than as a proton donor. However, an alternative possibility is that 2′-*O*-Me-ATP binds in a slightly different manner and thus retains some binding.

To resolve this question, we analyzed the complex of 2′-*O*-Me adenosine and the aptamer by NMR. The ATP derivative forms a well-defined complex at a 1:1 RNA:ligand ratio (0.5 mM), although it shows clear exchange peaks between free and bound ligand at 293 K, corresponding to a type (+) mutant aptamer. The analysis of the NOESY spectra revealed that the structure of the binding pocket remains unchanged. The 2′-*O*-Me group is located at the interface of the GNRA-motif and G17/G30 base-pair. It shows NOEs to A10 H2, G17 H1′, and its own H1′ as well as a weak interaction with C18 H1′ (see Figure 6). The only proton donors available in close proximity to the 2′ oxygen atom are G17 amino (which is involved in the G30·G17 base-pair) and U16 imino (Figure 7). The observed stacking arrangement and orientation of the 2′ oxygen relative to the base make G17 amino an unlikely candidate for an ATP interaction. The U16 has a fairly narrow imino resonance, indicative of slow exchange with the solvent. In addition U16 is the only highly conserved nucleotide without a clear role in the structure of

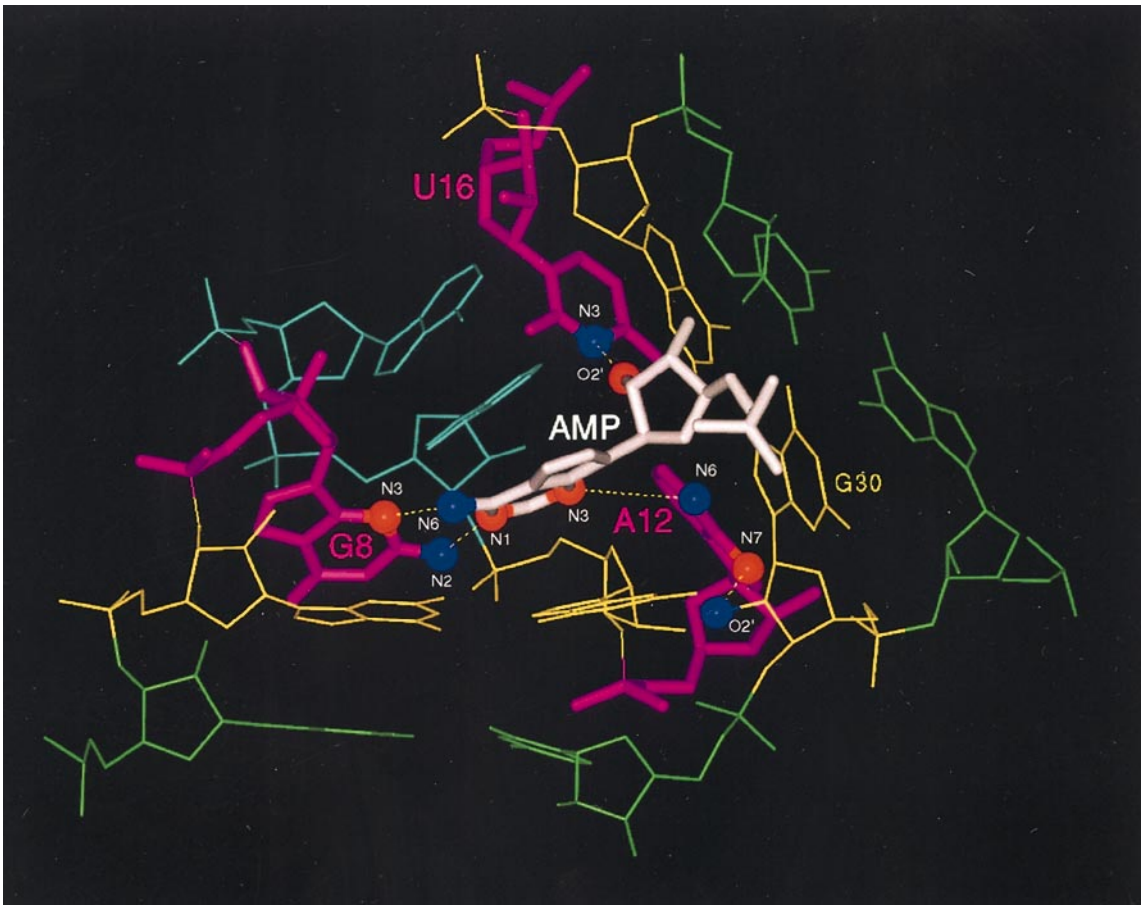

Figure 7. Three-dimensional structure of the core of the aptamer–AMP complex showing the hydrogen-bond interactions stabilizing the fold. Hydrogen bond donors and acceptors are labeled and shown as blue and red spheres, respectively. The coloring scheme is identical to that in Figure 2.

the complex. It should be noted that an alternative hydrogen bonding interaction between U16 imino and the A12 N1 is also possible. However, the observed chemical shifts for A12 N1, the intensity of the observed NOEs, and the relative orientation of the two bases relative to each other and the AMP do not provide experimental support for this interaction. The most likely interaction is between the AMP and U16, which are well oriented to form a hydrogen bond between the U16 imino proton and the 2′ O of the ligand.

Binding of AMP initiates formation of the binding pocket

The three-dimensional fold of the ATP-binding aptamer and its stability are to a large extent determined by the interactions of ligand and RNA. The adenosine moiety of the bound ATP provides the acceptors and donors for four essential hydrogen bonds in the core of the aptamer. It functions as the last nucleotide in the GNRA motif and forms two H-bonds with G8. In addition its N3 and 2′ hydroxyl interact with U16 and A12, thus providing the only interactions between the two halves of the binding pocket. Thus, the bound ligand is integral to the overall fold, and functions to connect the ''GNRA stem-loop'' (nt 1 to 11; AMP, 31 to 36) with the second helix. There is no evidence for any kind of binding pocket or defined structure of the internal loop in the absence of AMP.

Conclusions

The type of ligand-dependent folding found for the ATP-binding aptamer seems to be characteristic for all of the small molecule binding aptamers that have been investigated (Dieckmann *et al.*, 1996; Fan *et al.*, 1996; Feigon *et al.*, 1996; Jiang *et al.*, 1996b; Yang *et al.*, 1996). Thus it seems that, with respect to folding and design of cofactor binding aptamers, the most important question is how RNA and ligand can interact to form the most stable complex, rather than how the RNA can form a structure/pocket capable of recognizing the ligand. This is a remarkable difference compared to proteins where the ligand is generally recognized by a preformed binding pocket; i.e. the overall fold usually does not depend on the presence of the ligand, except for local changes due to

''induced fit''. The rational design of RNA–ligand interactions will therefore require approaches that take into account the properties of both the RNA and the ligand, and that do not rely solely on the RNA sequence and structure.

Materials and Methods

NMR sample preparation

The RNA was synthesized enzymatically on a DNA template using bacteriophage T7 RNA polymerase and unlabeled NTPs (Milligan *et al*., 1987). The labeled NMPs were isolated from methanolotrophic bacteria that had been grown on [^{13}C]methanol and [^{15}N]ammonia, purified, and converted to NTPs as described (Batey *et al*., 1992; Peterson *et al*., 1994). For selectively labeled samples, the mixture of NTPs was separated into the four nucleotides by HPLC using a semi-preparative scale C18 column (Waters: PrepPak Cartridge, 25 mm × 100 mm) with a water/methanol (0 to 100% linear) gradient. A specifically labeled sample of the G8A mutant was prepared using labeled [^{15}N,^{13}C]ATP and commercial, non-labeled GTP, UTP, and CTP. After enzymatic synthesis, the RNA was purified, and NMR samples were prepared as described (Dieckmann *et al*., 1996; Peterson *et al*., 1994). NMR samples of the mutant aptamers were typically 0.5 to 1.6 mM in RNA (pH 6.0), 100 mM NaCl. AMP for the NMR and binding studies was purchased from Sigma Chemicals, and the 2′-*O*-methyl-adenosine was a gift from Peninsula Laboratories, Inc.

Preparation of deoxyribose aptamer mutants

Mutant aptamers containing 2′ deoxynucleotide substitutions were chemically synthesized on a Milligen Cyclone Plus DNA synthesizer using ribonucleoside phosphoramidites (Chemgenes) and deoxyribonucleoside phosphoramidites (Chemgenes) at the desired positions. For the single deoxyribose substitutions, each aptamer was synthesized as two separate fragments, a 23-nucleotide oligonucleotide with the internal loop and an 11-nucleotide oligonucleotide containing the bulged G. The RNAs and RNA-DNA hybrids were deprotected as described (Whoriskey *et al*., 1995) and gel purified. The position of the 2′ deoxynucleotide substitution was confirmed by partial alkaline hydrolysis of the oligonucleotides followed by gel electrophoresis. The 23 nucleotide oligonucleotides were ^{32}P-end-labeled and annealed to a threefold excess of the unlabeled 11-nucleotide fragment for ATP–agarose column binding studies.

NMR spectroscopy

All NMR spectra were acquired at 500 MHz on Bruker DRX and AMX spectrometers. For spectra in 90% H_2O/10% ^2H_2O, pulse sequences with 11 spin-echo water suppression (Sklenář & Bax, 1987) were used. In the case of ^2H_2O samples the residual H^2HO resonance was suppressed by low-power presaturation. Quadrature detection for the indirect dimensions in multi-dimensional experiments was achieved using the States-TPPI method (Marion *et al*., 1989).

The binding properties of the mutant aptamers were qualitatively evaluated by titration of aptamer samples with AMP under standard solution conditions (100 mM NaCl (pH 6.0), $T = 274$ K) and observation of changes in the one-dimensional NMR spectra in 90% H_2O/10% ^2H_2O. In the case of samples that formed a stable complex (sample contains more than 90% RNA–AMP complex) a full set of two-dimensional NMR spectra including NOESY (Kumar *et al*., 1980), TOCSY (Bax & Davis, 1985) and DQF-COSY (Piantini *et al*., 1982) experiments was acquired. NOESY spectra in 90% H_2O/ 10% ^2H_2O were acquired at 274 K with mixing times of 150 and 300 ms. All other experiments were acquired in 100% ^2H_2O at 293 K. NOESY spectra were measured with mixing times of 80, 200 and 300 ms, and for TOCSY experiments mixing times of 50 to 80 ms were applied using CITY or DIPSI-2 (Shaka *et al*., 1985) sequences for the spin-lock. For the G8A mutant, additional NMR data were acquired using the A-labeled sample (Dieckmann & Feigon, 1997). Additional experiments performed on this sample were ^{1}H-^{13}C/^{15}N-HSQC (Santoro & King, 1992) and X-filtered NOESY (Otting & Wüthrich, 1990) experiments in ^2H_2O and H_2O measured under the same conditions as for the unlabeled sample.

All experiments on the 2′-*O*-Me-adenosine–RNA complex were carried out using a 0.5 mM sample of RNA in 100 mM NaCl at pH 6.0. The sample was titrated with the ligand up to a RNA:ligand ratio of ~1:2.5. DQF-COSY, NOESY and TOCSY spectra were acquired in 100% ^2H_2O and 90% H_2O/10% ^2_2O at 274, 278, and 293 K.

Column binding studies

The binding of the mutant aptamers containing base substitutions under *in vitro* selection conditions was studied by column binding experiments, essentially identical to those originally described (Sassanfar & Szostak, 1993). Samples of RNA (10 picomoles) from each of the NMR samples were 5′ end-labeled with ^{32}P using bacteriophage T4 polynucleotide kinase (USB) and [γ-^{32}P]ATP. Unincorporated ^{32}P was removed with a Sephadex G15 spin column. Aptamers were loaded on an ATP(C8)–agarose column (Sigma) in the binding buffer used in the original *in vitro* selection. Unbound RNA was washed from the column with 5.0 ml of binding buffer, followed by the elution of the bound RNA with 5 ml of binding buffer containing 4.0 mM ATP. Fractions (1 ml) were collected, and the amount of RNA in each fraction was estimated by measuring the amount of radioactivity (counts per minute). The binding of the aptamers containing deoxyribonucleotide substitutions was assayed as above except the buffer used was 300 mM KCl, 20 mM $MgCl_2$, 20 mM Tris-HCl (pH 7.6).

Measurement of apparent dissociation constants

The k_D values for mutant aptamers with substantial binding under NMR conditions were measured by isocratic elution from an ATP-affinity column. RNA from the NMR samples was 5′-labeled with ^{32}P. A 4.0 ml ATP(C8)–agarose column (ATP concentration 1.3 mM, void volume 3.1 ml) was equilibrated with buffer (300 mM NaCl, 5 mM MgCl, 20 mM Tris-HCl (pH 7.6)). The radiolabeled RNA was loaded on the column and eluted with buffer. Fractions (0.6 to 4.0 ml) were collected until the radioactivity of the fractions was back to the value of background radiation. The k_D was calculated using the equation:

$$k_D = [L]^*(V_t - V_0)/(V_e - V_0)$$

where $[L]$ is the concentration of ligand on the column, V_0 is the void volume of the column, V_t is the total

volume of the column, and V_e is the volume of buffer required to elute the RNA.

Molecular Modeling

Model structures of several mutant aptamers were generated based on the solution structure of the wild-type aptamer. For this purpose the coordinates of the lowest energy RNA–aptamer structure were edited using the InsightII software package (Biosym Inc.). The wild-type base was substituted by the mutant base, leaving the sugar conformation unchanged, and aligned by hand *via* a rotation around the χ angle to avoid steric clashes. This primary model was then energy minimized using the XPLOR 3.0 software package (250 steps using the energy terms for bonds, angles, impropers, and van der Waals interactions). In the case of mutants that clearly retained the overall wild-type fold (G7A, G8A, G17A) a minimum set of 369 NOEs not involving the substituted bases was used as additional constraints during the minimization. These NOE sets were based on the wild-type data set and checked against the NOESY data for each mutant.

Acknowledgments

T. D acknowledges a HFSPO long-term postdoctoral fellowship. S. E. B. is a Jane Coffin Childs Memorial Fund postdoctoral fellow. This work was supported by NSF grant MCB-9506913 and NIH grant GM37254 to J. F. We thank Mr Gerald Nakamura for the preparation of several mutant aptamers and Peninsula Laboratories for the gift of 6 mg 2′-*O*-methyl-adenosine.

References

Batey, R. T., Inada, M., Kujawinski, E., Puglisi, J. D. & Williamson, J. R. (1992). Preparation of isotopically labeled ribonucleotides for multidimensional NMR spectroscopy of RNA. *Nucl. Acids Res.* **20**(17), 4515–4523.

Bax, A. & Davis, D. G. (1985). MLEV-17-based two-dimensional homonuclear magnetization transfer spectroscopy. *J. Magn. Res.* **65**, 355–360.

Dieckmann, T. & Feigon, J. (1997). Assignment methodology for larger RNA oligonucleotides. Application to an ATP binding RNA aptamer. *J. Bio. NMR,* **9**, 259–272.

Dieckmann, T., Suzuki, E., Nakamura, G. K. & Feigon, J. (1996). Solution structure of an ATP-binding RNA aptamer reveals a novel fold. *RNA,* **2**, 628–640.

Ellington, A. D. & Szostak, J. W. (1990). *In vitro* selection of RNA molecules that bind specific ligands. *Nature,* **346**, 818–822.

Famulok, M. (1994). Molecular recognition of amino acids by RNA-aptamers: an L-citrulline binding RNA motif and its evolution into an L-arginine binder. *J. Am. Chem. Soc.* **116**, 1698–1706.

Fan, P., Suri, A. K., Fiala, R., Live, D. & Patel, D. J. (1996). Molecular recognition in the FMN-RNA aptamer complex. *J. Mol. Biol.* **258**, 480–500.

Feigon, J., Dieckmann, T. & Smith, F. W. (1996). Aptamer structures from A to ξ. *Chem. Biol.* **3**, 611–617.

Heus, H. A. & Pardi, A. (1991). Structural features that give rise to the unusual stability of RNA hairpins containing GNRA loops. *Science,* **253**, 191–194.

Jiang, F., Fiala, R., Live, D., Kumar, D. & Patel, D. J. (1996a). RNA folding topology and intermolecular contacts in the AMP-RNA aptamer complex. *Biochemistry,* **35**, 13250–13266.

Jiang, F., Kumar, R. A., Jones, R. A. & Patel, D. J. (1996b). Structural basis of RNA folding and recognition in an AMP-RNA aptamer complex. *Nature,* **382**, 183–186.

Jucker, F. M. & Pardi, A. (1995). GNRA tetraloops make a U-turn. *RNA,* **1**, 219–222.

Jucker, F. M., Heus, H. A., Yip, P. F., Moors, E. H. & Pardi, A. (1996). A network of heterogeneous hydrogen bonds in GNRA tetraloops. *J. Mol. Biol.* **264**, 968–980.

Kumar, A., Ernst, R. R. & Wüthrich, K. (1980). A two-dimensional nuclear Overhauser enhancement (2D NOE) experiment for the elucidation of complete proton-proton cross-relaxation networks in biological macromolecules. *Biochem. Biophys. Res. Commun.* **95**, 1–6.

Lauhon, C. T. & Szostak, J. W. (1995). RNA aptamers that bind flavin and nicotinamide redox cofactors. *J. Am. Chem. Soc.* **117**(4), 1246–1257.

Marion, D., Ikura, M., Tschudin, R. & Bax, A. (1989). Rapid recording of 2D NMR spectra without phase cycle. Application to the study of hydrogen exchange in proteins. *J. Magn. Reson.* **85**, 393–397.

Milligan, J. F., Groebe, D. R., Witherell, G. W. & Uhlenbeck, O. C. (1987). Oligoribonucleotide synthesis using T7 RNA polymerase and synthetic DNA templates. *Nucl. Acids Res.* **15**, 8783–8798.

Otting, G. & Wüthrich, K. (1990). Heteronuclear filters in two-dimensional [^{1}H,^{1}H]-NMR spectroscopy: combined use with isotope labelling for studies of macromolecular conformation and intermolecular interactions. *Quart. Rev. Biophys.* **23**(1), 39–96.

Peterson, R. D., Bartel, D. P., Szostak, J. W., Horvath, S. J. & Feigon, J. (1994). 1H NMR studies of the high-affinity Rev binding site of the Rev Responsive Element of HIV-1 mRNA: base-pairing in the core binding element. *Biochemistry,* **33**(18), 5357–5366.

Piantini, U., Sørensen, O. W. & Ernst, R. R. (1982). Multiple quantum filters for elucidating NMR coupling networks. *J. Am. Chem. Soc.* **104**, 6800–6801.

SantaLucia, J., Kierzek, R. & Turner, D. H. (1992). Context dependence of hydrogen bond free energy revealed by substitutions in an RNA hairpin. *Science,* **256**, 217–219.

Santoro, J. & King, G. (1992). A constant-time 2d overbodengausen experiment for inverse correlation of isotopically enriched species. *J. Magn. Reson.* **97**, 202–207.

Sassanfar, M. & Szostak, J. W. (1993). An RNA motif that binds ATP. *Nature,* **364**, 550–553.

Shaka, A. J., Barker, P. & Freeman, R. (1985). Computer-optimized decoupling scheme for wideband applications and low-level operation. *J. Magn. Reson.* **64**, 547–552.

Sklenar, V. & Bax, A. (1987). Spin-echo water suppression for the generation of pure-phase two-dimensional NMR spectra. *J. Magn. Reson.* **74**, 469–479.

Tuerk, C. & Gold, L. (1990). Systematic evolution of ligands by exponential enrichment: RNA ligands to bacteriophage T4 DNA polymerase. *Science,* **249**, 505–510.

Turner, D. H., Sugimoto, N., Kierzek, R. & Dreiker, S. D. (1987). Free energy increments for hydrogen bonds in nucleic acid base-pairs. *J. Am. Chem. Soc.* **109**, 3783–3785.

Whoriskey, S. K., Usman, N. & Szostak, J. W. (1995). Total chemical synthesis of a ribozyme derived from a group I intron. *Proc. Natl Acad. Sci. USA,* **92**, 2465–2469.

Yang, Y., Kochoyan, M., Burgstaller, P., Westhof, E. & Famulok, M. (1996). Structural basis of ligand discrimination by two related RNA aptamers resolved by NMR spectroscopy. *Science,* **272**, 1343–1347.

Edited by P. E. Wright

(Received 29 April 1997; received in revised form 25 July 1997; accepted 29 July 1997)